Recent advances and current challenges in magnetophoresis based micro magnetofluidics

Ahmed Munaz,[1] Muhammad J. A. Shiddiky,[1,2] and Nam-Trung Nguyen[1,a)]
[1]*Queensland Micro- and Nanotechnology Centre, Griffith University, Brisbane, QLD 4111, Australia*
[2]*School of Natural Sciences, Griffith University, Nathan Campus, QLD 4111, Australia*

(Received 15 April 2018; accepted 11 June 2018; published online 21 June 2018)

The combination of magnetism and microscale fluid flow has opened up a new era for handling and manipulation of samples in microfluidics. In particular, magnetophoresis, the migration of particles in a magnetic field, is extremely attractive for microfluidic handling due to its contactless nature, independence of ionic concentration, and lack of induced heating. The present paper focuses on recent advances and current challenges of magnetophoresis and highlights the key parameters affecting the manipulation of particles by magnetophoresis. The magnetic field is discussed according to their relative motion to the sample as stationary and dynamic fields. The migration of particles is categorized as positive and negative magnetophoresis. The applications of magnetophoresis are discussed according to the basic manipulation tasks such as mixing, separation, and trapping of particles or cells. Finally, the paper highlights the limitations of current approaches and provides the future perspective for this research area. *Published by AIP Publishing.* https://doi.org/10.1063/1.5035388

I. INTRODUCTION

Magnetophoresis is a phenomenon where particles migrate in a magnetic field. The phenomena can be further categorized as positive and negative magnetophoresis. Positive magnetophoresis is the migration of magnetic particles in a diamagnetic medium. Negative magnetophoresis is the migration of diamagnetic particles in a magnetic medium. Magnetophoresis occurs in a gradient of magnetic field, a gradient of magnetization of the surrounding medium, or the combination of both. The overall objective of magnetophoretic manipulation is the efficient handling of a large number of sample particles over a short period of time.[1,2] The magnetic permeability (μ), the magnetic flux density (B), and the susceptibility (χ) are the key parameters for designing and optimizing applications with magnetophoresis.[3] Magnetophoresis offers several advantages over other active methods for particle manipulation such as electrophoresis, thermophoresis, dielectrophoresis, optical trapping, and acoustophoresis.[4] Electrophoresis requires an electric field with direct electrode contact that may cause Joule heating and electrolysis. Thermophoresis needs a temperature gradient across the sample. Dielectrophoresis uses an electric field to affect the trajectory of particles in a fluid flow and may not need direct electrode contact to the liquid sample. However, the alternative current (AC) field could polarize biological cells and changes their metabolic function.[5] Optical actuation utilizes photon energy to move particles. The optical setup is usually complex and expensive. The heat generated by the focused laser beam could affect the behavior of sensitive biological particles and even kills them.[6] Acoustophoresis utilizes the pressure field or acoustic streaming often induced by a surface acoustic wave (SAW) to manipulate particles. An intense acoustic field may cause heat that is harmful to biological particles such as cells.[7]

a)Email: nam-trung.nguyen@griffith.edu.au. Tel.: +61 07 373 53921. Fax: +61 07 373 58021.

Magnetophoresis is a contactless method for manipulation of particles. This technique does not affect properties of the sample solution such as pH value, ion concentration, surface charge, and temperature. Furthermore, easy operation, low cost, and simple design make magnetophoresis a favorable option over other active manipulation techniques. The magnetic field can either be generated by a permanent magnet or an electromagnet. Permanent magnets provide a relatively strong magnetic field. But due to the size constraint, its magnetic field gradient is usually weaker than electromagnets that can be integrated on a chip with a relatively small footprint. Using tapered magnetic tips, small magnet arrays or magnetic poles can increase the magnetic field gradient by many folds.[8–10] Permanent magnets are suitable for portable point-of-care (POC) applications, where an external power source is not required. Furthermore, a setup with permanent magnets does not require any complicated fabrication process of the device. Magnetic fields have been successfully utilized for mixing, positioning, transport, and separation of magnetic and non-magnetic objects.[11] For some applications, a non-uniform magnetic field is necessary to create a strong magnetic field gradient. A large magnet relative to the microfluidic device can generate a quasi-uniform magnetic field that can magnetise the particles or the fluid but does not induce a net force acting on them.

Magnetic susceptibility of the particle and its surrounding medium is an important parameter for magnetophoresis. According to their magnetic susceptibility χ, materials are classified into ferromagnetic ($\chi \gg 0$), paramagnetic ($\chi > 0$), and diamagnetic ($\chi < 0$).[12] An object made of a ferromagnetic material is attracted towards a magnetic field. Iron, cobalt, and nickel are examples of ferromagnetic materials. Objects made of diamagnetic materials suspended in a paramagnetic medium are repelled from the magnetic flux maxima. Most biological samples such as proteins, cells, exosomes, and DNAs are diamagnetic. Paramagnetic materials such as oxygen, platinum, and manganese (II) salts are attracted towards the magnetic flux maxima. However, they lose their magnetism if the field is removed from the system. Red blood cells (RBCs) and magnetotactic bacteria are examples of paramagnetic objects found in nature.[13] Paramagnetic materials are further categorized into superparamagnetic materials such as iron oxides.[14] Paramagnetic particles behave like diamagnetic particles if the magnetic field is removed. A magnetic field can polarize these particles and change their trajectories in a fluid flow.[15] Antibodies or DNA strands can easily be immobilized on these particles for binding to and subsequently extracting targeted cells.

As mentioned above, the migration of particles in a magnetic field is categorized as positive and negative magnetophoresis according to the mismatch in magnetic properties of the particles and their surrounding medium. Positive magnetophoresis happens to paramagnetic particles suspended in a diamagnetic medium such as water. Positive magnetophoresis allows paramagnetic particles to accumulate at magnetic field maxima, enabling separation and mixing.[16] Positive magnetophoresis can be utilized for the manipulation and separation of biological samples specifically labelled by magnetic beads as tags.[17] Magnetic particles for labeling cells may have a size ranging from nanometers (Miltenyi Biotech: 50 nm, Estapor: 200 nm) to micrometers (BioMaagic/Biopal: 1.5 μm, Invitrogen/Dynabeads: 2.8 μm, 4.5 μm).[18] These magnetic particles offer flexible functionality, an augmented surface-volume ratio, and a controllable surface for manipulation of targeted biological molecules and cells.[19] Dynabeads are the most common superparamagnetic particles for applications utilizing magnetophoresis. Selecting the right nanoparticles for the intended application is crucial for successful use of magnetophoresis. For instance, nanometer-sized particles are suitable for labeling highly concentrated cells.[20] Micrometer-sized particles are more suitable for tagging rare cells such as circulating tumor cells (CTCs). Following tagging and trapping, cleaning steps are needed to release the biomolecules from the magnetic particles.[21,22] The release process is usually done by cell lysis and sample centrifugation that either change or damage the cells completely.

Negative magnetophoresis is a label-free approach for handling diamagnetic particles with a paramagnetic carrier fluid.[23] In a paramagnetic medium, diamagnetic particles with magnetic susceptibility χ_p serve as magnetic holes.[24] If the system is exposed to an external magnetic field gradient, the mismatch in magnetic susceptibility between the diamagnetic particle and the paramagnetic medium creates a negative magnetophoretic force that pushes the particles away

from the magnet.[25] A diamagnetic particle in a paramagnetic medium moves towards the magnetic field minima.[26] In this way, diamagnetic particles can be manipulated, mixed, and separated. Mixing and separation based on the size and shape can be implemented with negative magnetophoresis, because the magnetophoretic force is proportional to the volume of the particle.

A paramagnetic medium is essential for negative magnetophoresis. Some common paramagnetic fluids are ferrofluids (maghemite Fe_2O_3, or magnetite Fe_3O_4 nanoparticles suspended in a liquid) and paramagnetic salt such as manganese (II) chloride ($MnCl_2$) and diethylenetriamine pentaacetic acid (Gd-DTPA). It is noteworthy that ferrofluid has five times higher magnetic susceptibility than a highly concentrated paramagnetic salt solution.[27] However, the opaque nature of a ferrofluid makes visualization of the sample difficult. Therefore, fluorescent labeling of target cells is often needed for visualization and tracking purposes. Paramagnetic salt solutions offer optical transparency. However, due to their relatively low magnetic susceptibility, a highly concentrated paramagnetic salt solution is needed for effective negative magnetophoresis. The high salt concentration might destroy the cells due to osmosis. Therefore, selecting the right paramagnetic medium for an application is extremely important. Interestingly, positive and negative magnetophoresis could coexist in the same system. A paramagnetic particle could show diamagnetic behavior if the surrounding fluid is tuned into a stronger paramagnetic solution, for instance by increasing the concentration of the magnetic nanoparticles in a ferrofluid. Thus, the magnetic susceptibility of the carrier fluid can be adjusted to above or below that of the sample particles. Liang *et al.* used diluted ferrofluid instead of a diamagnetic medium in a T-shaped microchannel for the separation of magnetic and diamagnetic particles. The diluted ferrofluid improved the separation performance up to 60%.[28] Magnetic particles experience positive magnetophoresis and move towards the magnetic field maxima ($M_{p>}M_f$), while diamagnetic particles experience negative magnetophoresis and move towards magnetic field minima resulting in more efficient separation.

Figure 1(a) provides an overview of magnetophoresis-based micro magnetofluidics. The phenomena are classified by the dynamic nature of the external magnetic field. Both static and dynamic magnetic fields can induce positive and negative magnetophoresis. A dynamic magnetic field can be generated by a moving permanent magnet or a controllable electromagnet. Generally, a permanent magnet can be moved by an external electric motor to create a dynamic magnetic field. Electromagnets, for instance in the form of solenoids, can be driven by an AC current and generate a dynamic magnetic field. The strength of the field is adjusted by controlling the amplitude and frequency of the current source. Both positive and negative magnetophoresis using dynamic magnetic fields have been reported. Applications of magnetophoresis include spreading, focusing, mixing, trapping, and separation of fluids and particles, Fig. 1(b). For efficient separation, particle focusing is required. The focusing techniques can be further classified as sheath-based and sheath-free focusing. Spreading and mixing have been mostly

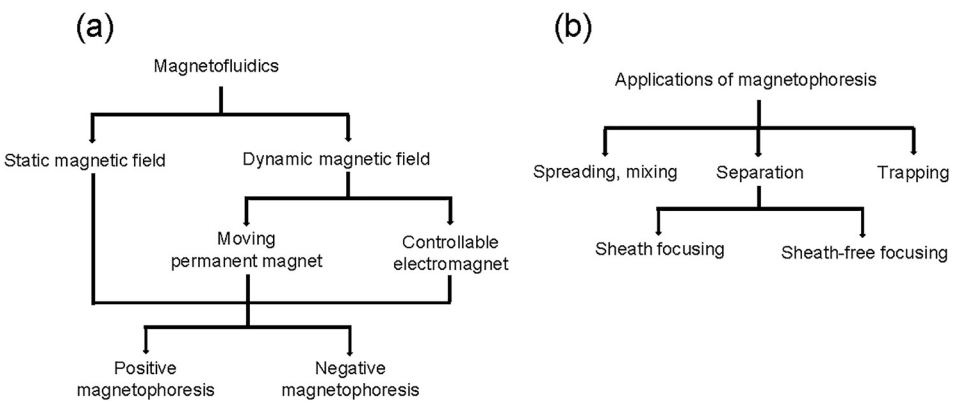

FIG. 1. Overview of magnetophoresis based magnetofluidic schemes (a) and applications (b).

reported for dynamic magnetic fields. The present review paper highlights the recent advancements of magnetophoresis based mixing, separation, and trapping of biological cells, magnetic beads, and fluorescent particles. Current challenges are thoroughly discussed. Finally, the paper provides the future perspective of magnetophoresis-based micro magnetofluidics.

II. FUNDAMENTAL AND THEORY OF MAGNETOPHORESIS

Magnetophoresis relies on the magnetization of a material under an external magnetic field, which is characterized by its magnetic susceptibility. The relationship between the magnetic field and magnetization is represented by

$$\nabla \mu_0(\mathbf{H} + \mathbf{M}) = 0, \tag{1}$$

$$\mathbf{H} = -\nabla V_m, \tag{2}$$

where $\mu_0 = 4\pi \times 10^{-7}$ is the permeability of the air, $\mathbf{H}$ is the magnetic field strength, $\mathbf{M}$ is the magnetization of the particle, and V_m represents the scalar magnetic potential.[29] As the magnetic force induced by magnetophoresis has to work against the inertial force and the drag force, magnetophoresis also depends on the fluid flow and the properties of the surrounding fluid such as the density and viscosity. Under the steady state condition, the flow field is described for the incompressible fluid medium surrounding the particles by the continuity equation[2]

$$\nabla.(\rho_f \mathbf{u}_f) = 0, \tag{3}$$

where ρ_f is the density of the fluid and $\mathbf{u}_f$ is the velocity of the fluid; and the Navier-Stokes equation

$$p_f(\mathbf{u}_f.\nabla)\mathbf{u}_f = -\nabla P + \nabla.(\eta.\nabla \mathbf{u}_f), \tag{4}$$

where P is the pressure and η is the dynamic viscosity of the fluid.[30] The migration of particles under an external magnetic field depends on the balance of forces acting on it.[31] The main forces acting on the particle are the inertial force ($m_p d\mathbf{v}/dt$), the magnetic force $\mathbf{F}_\mathrm{m}$, and the fluid drag force $\mathbf{F}_\mathrm{d}$. For a shallow channel and an incompressible fluid, gravitational force $\mathbf{F}_\mathrm{g}$, Brownian force $\mathbf{F}_b$, and the particle lift force $\mathbf{F}_\mathrm{l}$ are negligible. The force balance is represented by

$$m_p \frac{d\mathbf{v}}{dt} = \mathbf{F}_m + \mathbf{F}_d, \tag{5}$$

where m_p is the mass of the particle, v is the velocity of the particle, $\mathbf{F}_\mathrm{m}$ is the magnetic force, and $\mathbf{F}_\mathrm{d}$ is the viscous drag force. According to the Stokes law, the viscous drag force is determined as

$$\mathbf{F}_d = \frac{1}{\tau_p} m_p(\mathbf{u}_f - \mathbf{v}), \tag{6}$$

where τ_p (s) is the velocity response time of the particle

$$\tau_p = \frac{\rho_p d_p^2}{18\mu}, \tag{7}$$

where ρ_p and d_p are the density and the diameter of the particle, respectively; μ is the fluid viscosity. For a given particle size, the drag force can be adjusted by the velocity, the density, and

the viscosity of the fluid. The magnetic force acting on a particle suspended in a fluid medium is

$$\mathbf{F}_m = \frac{V(\chi - \chi_m)}{\mu_0}(\nabla.\mathbf{B})\mathbf{B}, \tag{8}$$

where V is the particle volume, χ is the magnetic susceptibility, χ_m is the susceptibility of the surrounding medium, μ_0 is the magnetic permeability of the air, and $\nabla.\mathbf{B}$ represents the field gradient of the magnetic flux density $\mathbf{B}$. Magnetic force is determined by the size of the magnet, its strength, its distance from the channel, and the orientation of the magnetization. Effective manipulation of particles requires a strong magnetic field gradient, which can be implemented using special magnet geometry, an array of magnets, integrated micro electromagnets, or ferromagnetic wire array.[2] Positive and negative magnetophoresis is determined by the susceptibility of the particle and its surrounding fluids.

III. APPLICATIONS OF MAGNETOPHORESIS

Magnetophoretic manipulation of particles and cells depends on their magnetic and geometric parameters as well as that of the flow system. Parameters such as flow rate, viscosity, magnetic field strength, magnetic susceptibility of the fluid, and the particle size are essential for optimizing this manipulation concept.[32] Geometric parameters such as the size and shape of the permanent magnet, distance of the magnet from the channel, and orientation of the magnetization define the magnetic field and its gradient, thus directly affecting the performance of magnetophoretic manipulation. Optimizing these parameters can tune magnetophoretic manipulation to suite a wide range of applications such as the disease diagnosis, therapeutics, environmental monitoring, genetic engineering, cell sorting, and single cell investigation.[5,33]

Mixing of samples is an important task for many applications including chemical analysis, *in-vitro* drug testing, labeling magnetic beads, and specific binding of target molecules.[34] Applications of mixing in chemical engineering include synthesis of material, crystallization, polymerization, and extraction. Applications of mixing in bioengineering are protein folding, enzymatic assay, cell lysis, and DNA analysis.[35] Efficient mixing and subsequent separation and detection steps in a lab-on-a-chip (LOC) device allow for the development of fully automated devices. Table I lists the basic specifications of recently reported devices for mixing by magnetophoresis. Efficient mixing above 80% has been observed in most of the reports. Both static and dynamic magnetic fields have been used. Flow rates, concentration, rotational speed, and frequency are the most key parameters for the mixing process. The details are discussed in Sec. A.

The separation of beads bound to targeted biomolecules is another important task in chemical synthesis, biochemical analysis, and monitoring and prevention of foodborne bacteria.[7] Separation of diseased cells such as circulating tumour cells or malaria-infected red blood cells from the healthy cells in a blood sample is another important application of magnetophoretic separation. Table II lists the recent applications of separation by magnetophoresis. Efficient separation can be done with both positive and negative magnetophoresis. Diamagnetic cells are labeled with magnetic beads for the separation with positive magnetophoresis. A static magnetic field is essential for the separation. Details are discussed in Sec. B.

Trapping is another form of separation that often is the final sample preparation step. The trapped cells or cell clusters can be used for further culture and drug testing. Trapped cells can further be cultured and assembled into a tissue. Trapping and concentrating cells in a specific region allows for the investigation of cell-cell interactions and their regulation mechanism.[36] On-chip trapping and concentration of target cells save reagent in use, avoid off-chip washing, and minimize the sample loss. Consequently, the accuracy of the assay is improved with reduced time and cost.[37] Table III lists the recent applications of trapping with magnetophoresis. Target cells were isolated and trapped into magnetic field maxima and minima according to their size and magnetic susceptibility. Details are discussed in Sec. C.

TABLE I. Mixing with magnetophoresis.

Source of mixing	Optimized parameters	Sample mixing	Size of particle (diameter)	No. of flow stream	Magnetophoresis	Mixing Performance (%)	References
AC electromagnet	Amplitude, frequency, flow rate ratio	Ferrofluid with mineral oil	10 nm	3	Negative	95	44
Permanent magnet	Flow rate ratio	Ferrofluid with glycerol-water	10 nm	3	Negative	…	46
Permanent magnet	Flow rate ratio, binding ratio	Magnetic beads with DNA strands	2 μm	3	Positive	…	43
Permanent magnet	Flow rate, concentration	Ferrofluid with DI water	10 nm	2	Negative	88	49
Embedded electrode	Switching frequency	Magnetic beads with biomolecules	1-1.4 μm	2	Positive	…	52
AC electromagnet	Frequency, channel width	Magnetic particle, DI water	1-1.4 μm	2	Positive	97.7	53
Modified magnetic stirrer	RPM, flow rate	Magnetic particle with fluorescent	4 μm	3	Positive	96	54
Electrode stripes	Switching frequency, flow rate, nanoparticle size	Magnetic nanoparticle with target biomolecules	50-300 nm	1	Positive	100	58
AC electromagnet	Amplitude, frequency, flow rate	Magnetic beads with fluorescein solution	Mean diameter 3 μm	2	Positive	95	59
Rotational permanent magnet	RPM, flow rate	Polystyrene beads with ferrofluid	30 μm	2	Negative	88	61
Magnetic stirrer	RPM, position of the actuator	Rifampicin drug with TiO_2 nanoparticle	…	2	Positive	90	62

TABLE II. Separation with magnetophoresis.

Source of separation	Optimized parameters	Sample separation	Size of particle (diameter)	No. of flow stream	Magnetophoresis	Separation efficiency (%)	Reference
Permanent magnet	Flow rate	Dynabeads	2.8 μm, 4.5 μm	2	Positive	100	8
Permanent magnet, micro-slit filter	Flow rate, magnet position	CTCs from whole blood	15-25 μm	1	Positive	Above 80	22
Permanent magnet, hydrodynamic filter	-	Human lymphocyte cells labeled with magnetic beads	13.2±3.9 μm	2	Positive	Above 90	67
DC electromagnetic wire array	Current, flow rate, concentration	Labeled MCF-7 from the Raji-B-lymphocyte cells	20-24 μm	2	Positive	Above 85	68
Permanent magnet	Flow rate	Yeast cells from polystyrene particle	3, 10 μm	1	Negative	…	72
Permanent magnet	flow rate, concentration of cells	CTCs from RBC lysed blood	15.5-18.9 μm	1	Negative	92.9	74
Permanent magnet	Magnetic volume fraction, flow rate	Magnetic beads, polystyrene beads	2.8 from 8.2 μm, and 2.6 from 4.2, 7.3, 7.9 μm	1	Positive/negative	…	17
Permanent magnet with nickel structures	Concentration	U937 from RBCs, polystyrene beads	10 from 6 μm, and 8 from 10 μm	2	Negative	90	79
Permanent magnet with nickel wires	Flow rate	i-RBCs from the h-RBCs	…	3	Positive	98.3	80
Permanent magnet with angled ferromagnetic wire	Concentration, flow rate	Labeled CTCs from whole blood	15-25 μm	2	Positive	90	81
Permanent magnet	Flow rate, magnet position, concentration	Seven cancer cell lines from WBCs	…	3	Negative	82.2	83

TABLE III. Trapping with magnetophoresis.

Source of trapping	Optimized parameters	Sample trapped	Size of particle (diameter)	No. of flow stream	Magnetophoresis	Trapped efficiency (%)	References
Permanent magnet, iron beads	Magnetic field strength, time	Magnetic nanoparticle	30 nm	3	Positive	…	41
Electromagnetic nickel wires and nickel pattern	Flow rate, concentration	S. Typhimurium labeled nanoparticle	2-5 μm	2	Positive	…	90
Permanent magnet	Flow rate	Magnetic beads, THP-1 labeled Dyna beads	8-10 μm, 10$\pm$1.5 μm	1	Positive	62	91
Permanent magnet	Flow rate, concentration	Polystyrene beads	3.2, 4.8 μm	1	Negative	…	93
Permanent magnet	Concentration	Polystyrene beads, yeast, algae	2.5-6 μm, 3-4 μm	1	Negative	…	94
Permanent magnet	Magnetic field, duration, flow rate	Bacteria, polystyrene beads	L$\times$W: 10 $\times$ 4.5 μm	1	Negative	…	36 and 95
Permanent magnet	Flow rate, duration	polystyrene beads, magnetic particle	9.9, 2.8 μm	1	Positive/ negative	…	96
Permanent magnet	Flow rate, magnet distance, duration	polystyrene beads, yeast cells	5 μm, 3-4 μm	1	Negative	…	98
Permanent magnet	Magnetic setup, flow rate, duration	polystyrene beads	5 μm	1	Negative	…	99
Rotating magnets	Geometry of magnets, flow rate, RPM, Concentration	Magnetic beads, E.coli	6.5 μm, L$\times$W: 0.5 $\times$ 2 μm	1	Negative	…	101

Figure 2 provides an overview of possible magnetophoretic effects that can be utilized for mixing, separation, and trapping. Figure 2(a) shows the typical scenario of positive magnetophoresis, where two types of magnetic particles are separated in a magnetic field due to the size difference. Figure 2(b) illustrates the separation of diamagnetic particles by negative magnetophoresis. Both the positive and negative magnetophoresis can coexist if the magnetic susceptibility of the surrounding fluid lies between those of the two particle types, Fig. 2(c).

A. Magnetophoresis for mixing

The use of magnetic force for mixing of fluids has attracted considerable attention due to its contactless and non-invasive nature. Independence of ion concentration as well as temperature and the low cost are some of the unique advantages of magnetic mixing.[3] As the sample flow is laminar in most microfluidic devices, the external magnetic energy ensures that particles and fluids gain enough energy to overcome viscous forces in the small scale.[38,39] Figures 3–5 show examples of recent device design for mixing using magnetophoresis.

Mixing of particles and cells can be implemented by placing a stationary magnetic field around the mixing chamber. In this system, magnetic particles (positive magnetophoresis) or a paramagnetic fluid (negative magnetophoresis) can be manipulated for mixing. A stationary magnetic field is generated by either an electromagnet or a permanent magnet. Compared to permanent magnets, an electromagnet usually provides a weaker magnetic field and consequently a smaller magnetic force acting on the particles.[12,14] The field and the force induced by an electromagnet can be increased with more turns in the coil and a higher supplied current. Microcoils integrated into the LOC can be used for both actuating and sensing the sample fluids. For instance, Kong and Nguyen used a liquid metal microcoil as a sensor to detect the hematocrit level of blood .[40] Actuating capabilities of the microcoil embedded in an adhesive membrane have been investigated for the potential use of micropumps. Interaction of an AC current and the magnetic field from a permanent magnet induced a magnetic force to oscillate the membrane. Soft magnetic microstripes have been integrated into the microfluidic device to focus the magnetic field and to increase its gradient.[12] Soft magnetic materials such as iron, nickel, or permalloy have been reported to increase the local magnetic field gradient.[41,42]

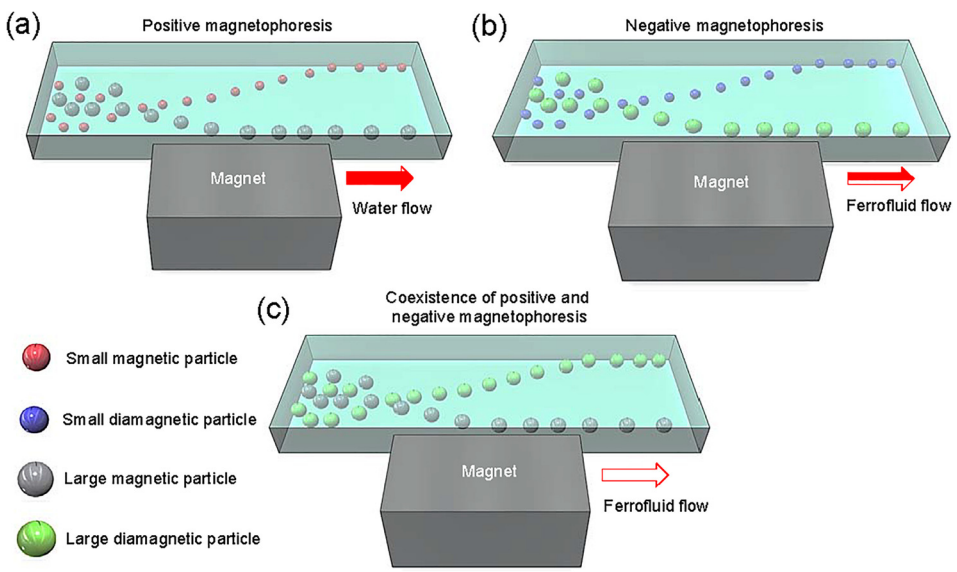

FIG. 2. Effects of magnetophoresis in a microchannel based on the size and magnetization for (a) positive magnetophoresis, (b) negative magnetophoresis, and (c) the coexistence of positive and negative magnetophoresis. Paramagnetic fluid such as ferrofluid or the salt solution is essential to initiate negative magnetophoresis. The susceptibility of the paramagnetic solution needs to be in between the susceptibility of the sample particles for the coexistence.

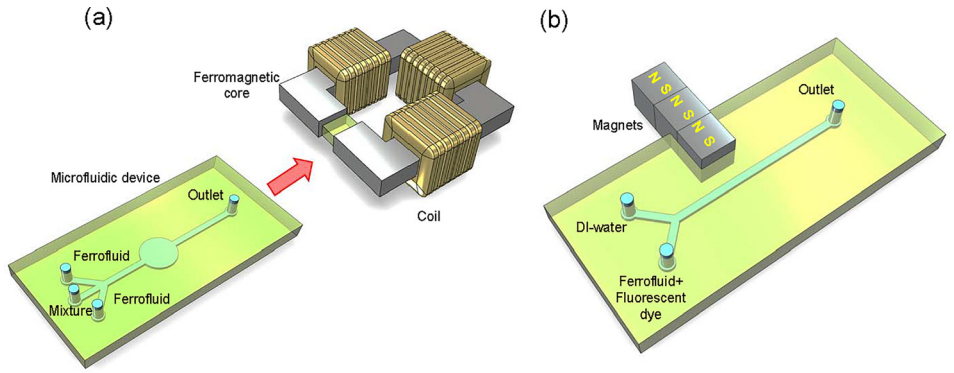

FIG. 3. Mixing in microfluidics (a) spreading of the ferrofluid under an external electromagnetic fields. Reproduced with the permission from G.-P. Zhu and N.-T. Nguyen, Lab Chip **12**, 4772–4780 (2012). Copyright 2012 The Royal Society of Chemistry. (b) Deflection of the ferrofluid towards the magnet. Reproduced with the permission from M. Hejazian and N.-T. Nguyen, Micromachines **8**, 37 (2017). Copyright 2017 Molecular Diversity Preservation International and Multidisciplinary Digital Publishing Institute. (Figures are not to scale.).

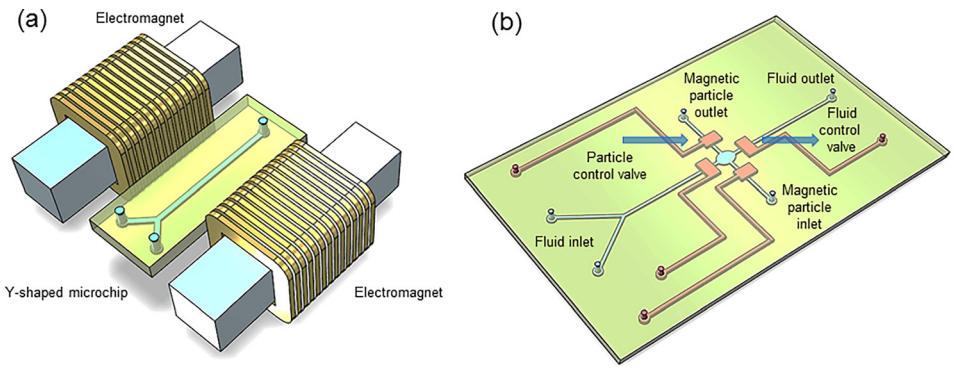

FIG. 4. Mixing in microfluidics (a) Y-shaped microchip placed between a time-dependent current carrying electromagnets. Reproduced with the permission from Wang *et al*., Microfluid. Nanofluid. **4**, 375–389 (2008). Copyright 2008 Springer-Verlag. (b) Microchip placed on top of a magnetic stirrer. The pressure controlled pneumatic valves (red lines) are on top layer of the microchannel (blue lines). Reproduced with the permission from Lee *et al*., Lab Chip **9**, 479–482 (2009). Copyright 2009 The Royal Society of Chemistry. (Figures are not to scale).

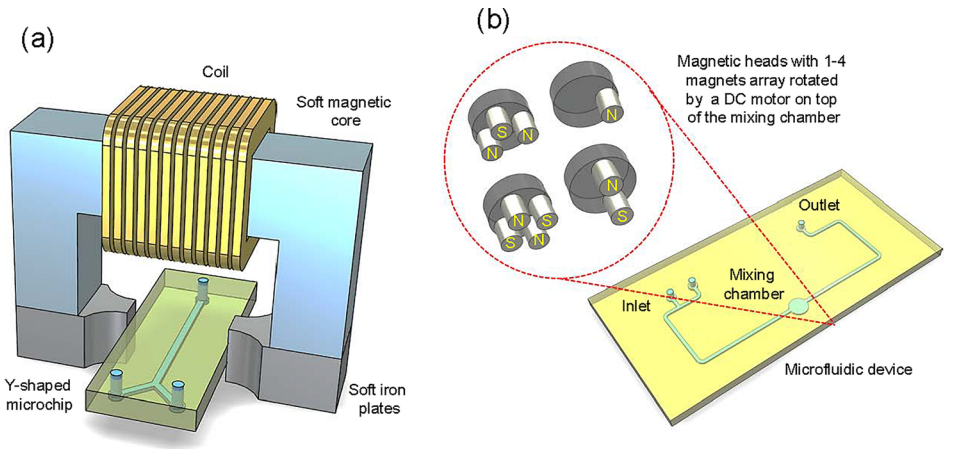

FIG. 5. Mixing in microfluidics (a) Y-shaped micromixer placed in an external electromagnetic assembly. Reproduced with the permission from A. Rida and M. Gijs, Anal. Chem. **76**, 6239–6246 (2004). Copyright 2004 American Chemical Society. (b) Magnetofluidic mixing by rotational magnetic field. Reproduced with the permission from Munaz *et al*., RSC Adv. **7**, 52465–52474 (2017). Copyright 2017 The Royal Society of Chemistry. (Figures are not to scale).

Different fabrication approaches such as photolithography, etching, sputter deposition, and polymer photoablation have been used for the fabrication of these structures.

The fabrication of soft magnetic structures and microcoils could be complex. In the case of an integrated electromagnet, the increased temperature in the microchannel may lead to undesirable sample damage.[43] Zhu and Nguyen investigated the fundamental spreading phenomenon of a ferrofluid core stream sandwiched between two diamagnetic streams in the uniform field of an electromagnet.[44] The induced magnetic force on the ferrofluid generated a secondary bulk flow that spreads the ferrofluid into the cladding diamagnetic streams. Various flow rate ratios were investigated to optimize the spreading performance. Zhu and Nguyen later utilized the same setup to investigate the mixing effects of water-based ferrofluid with a solution of deionized water (DI water) and glycerol, Fig. 3(a).[45] The roles of the magnetic flux density, flow rate, and viscosity ratio were analysed and optimized for higher mixing efficiency. Wang *et al.* studied the spreading of ferrofluid in a three-stream configuration,[46] consisting of a water-based ferrofluid stream sandwiched between two diamagnetic streams. A strong magnetic field, a low flow rate, and a high concentration of the ferrofluid promote the spreading phenomenon. Lund-Olesen *et al.* integrated a number of soft-magnetic structures that were magnetised by an external electromagnet.[47] The structures retain magnetism after removing the magnetization source and are able to trap a plug of magnetic beads inside of the microchannel. These beads move in a circular path and initiate mixing between two co-flowing fluid streams with a relatively low actuating magnetic field. The mixing efficiency depends on the geometry and the position of the integrated soft magnets.

For mixing with positive magnetophoresis, the particle size is an important factor. Large particles may aggregate in the channel, clogging the flow path and making mixing more difficult. A higher concentration of particles also leads to the same problems. Ganguly *et al.* demonstrated immunochemical binding of the magnetic beads with short DNA strands through mixing using an external permanent magnet.[43] The transverse magnetic field transports streptavidin-coated magnetic particles across a co-flowing stream of the biotinylated probe oligonucleotide. Similarly, Tarn *et al.* reported rapid coating of a polymer layer on magnetically modified live yeast cells in a microfluidic device.[48] The modified cells were sequentially deflected towards the co-flowing polyelectrolyte solution and washing buffer for coating and cleaning, respectively. A rectangular permanent magnet was used to induce magnetophoresis in the device. This method suits well for the low-cost and convenient fabrication of multilayered capsules and biosensors for genotoxicity and cytotoxicity.

Mixing and magnetophoresis of magnetic nanoparticles and subsequently induced magneto-convective secondary flow have also been reported. For instance, Hejazian and Nguyen reported mixing of ferrofluid and water streams in a non-uniform magnetic field, Fig. 3(b).[49] Susceptibility mismatch between the two streams induced magnetoconvection. Mixing efficiency was evaluated for a range of flow rates and ferrofluid concentrations. An optimum flow rate of 45 μl/min and a ferrofluid concentration of $\varphi = 20\%$ vol. offered a maximum mixing efficiency of 88%.

Mixing of diamagnetic particles can be implemented with negative magnetophoresis. Zhu *et al.* demonstrated the spreading of ferrofluid and the migration of 1-μm diamagnetic polymer particles in a uniform magnetic field.[23] The ferrofluid stream was sandwiched between two diamagnetic streams. Different flow rate ratios, magnetic field strengths, and ferrofluid concentrations were investigated. Tsai *et al.* studied the effects of the shape and geometry for the distribution of ferrofluid in water in the field of an external permanent magnet.[50] The Y-shaped geometry can increase the mixing efficiency up to 90%. In this work, the permanent magnet was placed under the microfluidic chip. Mixing efficiency was optimized for different flow rates, lengths, and widths of the channel. Nouri *et al.* conducted similar experiments to investigate mixing of ferrofluid and water in a Y-shaped microchannel.[51] Increasing the field strength of the magnet, increasing the concentration of nanoparticles, and decreasing the flow rates led to an improved mixing performance. A permanent magnet adjacent to the microchannel could yield a maximum mixing efficiency of almost 90%.

In some applications with low diffusivity of relatively large particles such as DNAs, protein molecules, or cells with target antigen-antibody, the time and required length of the

microchannel are not always sufficient for complete mixing with a stationary magnetic field. Larger particles such as blood cells and bacteria have an even much lower diffusion coefficient. In this case, a dynamic magnetic field is needed to enhance mixing. The external permanent magnet can move in a circular or linear path to initiate mixing in a microchamber. An electromagnet can also induce a time-dependent and tunable magnetic field gradient for magnetophoresis-based mixing. A dynamic, moving magnetic field introduces an extra inertial force into the force balance and enhances the migration of the particles allowing them to follow the moving magnetic field. The speed of the permanent magnet and the switching frequency of the electromagnet affect both inertial force and friction force and are important parameters for optimizing the mixing performance. Similar to the case of a stationary field, other parameters such as magnetic field strength, flow rate, and dimension of the microchannel also play a role in optimizing the mixing performance.

Suzuki *et al*. developed a microcoil as a source of dynamic magnetic field to induce the mixing process.[52] Stretching and folding of fluids were observed in the serpentine channel geometry, while the time-dependent magnetic field was activated. A sample with biomolecules was mixed with suspended magnetic bead for antigen-antibody binding. Wang *et al*. developed a simple micromixer using a pair of electromagnets, Fig. 4(a).[53] Mixing was enhanced by dynamically altering the magnetic field that moves the magnetic particles in the fluid. The agitation of magnetic particles led to a mixing efficiency of 97.7%. Mixing events were affected by the geometry of the electromagnet, switching frequency, magnetic field strength, and channel width of the device.

Lee *et al*. used a commercial stirrer to initiate mixing of two fluids by introducing ferromagnetic particles into a microchannel, Fig. 4(b).[54] A solution with 1% w/v of 4-μm ferromagnetic particles allowed for optimal mixing without clogging the channel. The magnetic beads formed a rod-like structure and aligned with the rotating magnetic fields. This configuration led to a mixing efficiency of 96% within a short distance. Ryu *et al*. fabricated a Permalloy rotor of 400-μm diameter in a 420-μm Polydimethylsiloxane (PDMS) based microchamber.[55,56] The rotation was initiated by a conventional stirrer plate for mixing of two types of dyes. The mixing index was 0.045 or a mixing efficiency of 95.5% at 150 rpm indicating efficient mixing 3 mm downstream of the stir bar. Oh *et al*. reported a configuration with two parallel channels intersecting the T-shaped mixing channel.[57] Ferrofluid slugs were oscillated in the subchannel by moving external permanent magnets. The movement of the magnets along the microchannel is controlled by a DC motor. The ferrofluid actuator promoted chaotic advection in the main flow channel. Munir *et al*. utilized a periodic magnetic force to oscillate magnetic nanoparticles.[58] An array of conductor stripes at the bottom of the microchannel generate the dynamic magnetic field gradient. A range of inlet velocities, nanoparticle sizes, and switching frequencies was investigated to optimize the mixing process. Rida and Gijs also used the dynamic motion of ferromagnetic beads to initiate mixing, Fig. 5(a).[59] The beads assembled themselves in a chain between two soft-ferromagnetic plates. The plates connected to an external electromagnet that focused the magnetic field locally. The frequency and magnitude of the dynamic field can be tuned. The team reported a mixing efficiency of almost 95% between a fluorescent stream and a non-florescent stream. Biswal and Gast demonstrated mixing of acid and base fluids with the aggregated chain of paramagnetic particles.[60] The binding and stability of the chain were ensured by linking the streptavidin-coated paramagnetic particles with the biotinylated poly(ethylene glycol) (PEG) molecules. The rotational magnetic field was introduced by two pairs of coils. The bead chain circulated with the moving field.

Munaz *et al*. demonstrated efficient mixing using negative magnetophoresis, Fig. 5(b).[61] The rotational magnetic field was generated by arranging a number of cylindrical permanent magnets on a rotating plate. The orientation of the magnets, the rotation speed, the magnetic field strength, and the flow rate ratio were investigated for optimum mixing. A mixing efficiency of 86% was achieved for 30-μm diamagnetic particles suspended in a ferrofluid solution of only 1% vol. concentration. Veldurthi *et al*. investigated magnetic actuator based mixing of rifampicin drugs (RIF) with titanium dioxide (TiO_2) nanoparticles.[62] A conventional magnetic stirrer was used to induce the dynamic magnetic field. The model was optimised by numerical

simulation and further validated by mixing dyes at different rotational speeds. The same setup was used in another work to infuse the Benzathine Penicillin G Tetrahydrate (BPG) into TiO_2. The synthesised drug nanocomplexes (DNC) were collected at the outlets.[63] The produced DNC effectively annihilated the S. aureus bacteria representing the effectiveness of the mixing process. Owen *et al*. showed a novel approach toward mixing using an array of rotating magnetic microbeads (2.8 μm, Dynabeads).[64] The microchannel was patterned with an array of soft magnetic permalloys and magnetized by the external magnets. The microbeads are attracted to the poles and follow the external magnets. Mixing was evaluated for the two co-flowing fluids. Azimi and Rahimi showed the stimulation of a two-phase flow under static and rotational magnetic fields.[65] Fe_3O_4 nanoparticles were loaded into a T-micromixer and the stimulation behavior of organic (n-butanol) and aqueous (succinic) solvents was investigated. Mixing characteristics were investigated for a range of ferrofluid concentrations, RPM, and field strengths of the magnets. The rotational magnetic fields showed better mixing compared to the static magnetic field. The above examples indicate that a dynamic magnetic field improves mixing compared to a stationary magnetic field. However, a setup with dynamic magnetic field is relatively complex, and the mixing protocol needs to be optimized carefully according to the targeted application.

B. Magnetophoresis for separation

Particle and cell separation from a mixture is an important sample preparation task. High throughput and efficient separation depend on the parameters of the device, properties of the particles, and the surrounding medium. Device parameters are the geometry and dimension of the microchannel, size and shape of the magnets, the strength of the magnet, and their distance from the channel.[32] The properties of particles and fluid include the concentration, fluid viscosity, and magnetic susceptibility. The majority of reported separation of particles and cells using magnetophoresis is based on their difference in size and shape. Figures 6–8 show some of the recent devices for separation of particles and cells using magnetophoresis.

Pamme *et al*. reported continuous separation of superparamagnetic particles with diameters of 2.8-μm and 4.5-μm.[8] A simple permanent magnet positioned perpendicular to the fluid flow allowed the separation of particles based on their size and magnetic susceptibility. To separate diamagnetic particles such as cells with positive magnetophoresis, they should be first tagged with magnetic particles. Mouse macrophage and HeLa cells were tagged with magnetic nanoparticles for separation in an external magnetic field.[18] The flow rate, magnetic field strength, the size of the cells, and the incubation time were the major parameters determining the separation efficiency. Positive magnetophoresis allowed for the isolation of specific targets as low as

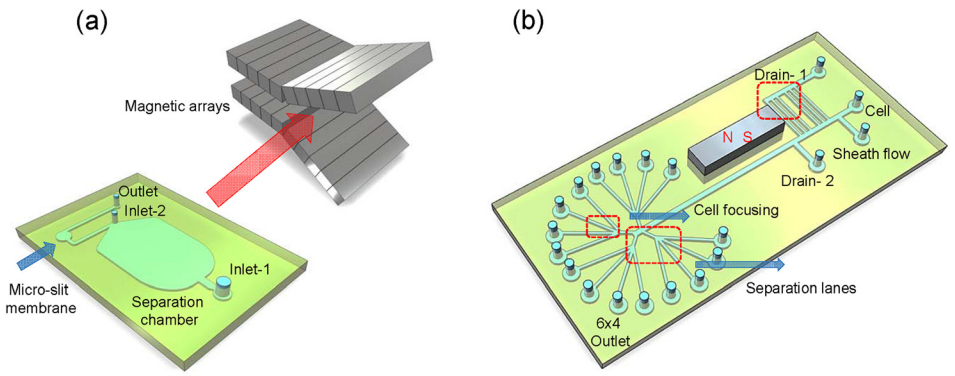

FIG. 6. Separation in microfluidics (a) CTC isolation chip. Module 1 promotes an immunomagnetic separation for WBCs, and Module 2 allows size based separation to retain CTCs. Reproduced with the permission from Gourikutty *et al*., J. Chromatogr. B **1011**, 77–88 (2016). Copyright 2016 Elsevier B.V. (b) Cell sorting system with the combination of hydrodynamic filtration (HDF) and magnetophoresis. In magnetophoresis, cells are first focused and then separated based on the size and surface market expressions. Reproduced with the permission from Mizuno *et al*., Anal. Chem. **85**, 7666–7673 (2013). Copyright 2013 American Chemical Society. (Figures are not to scale).

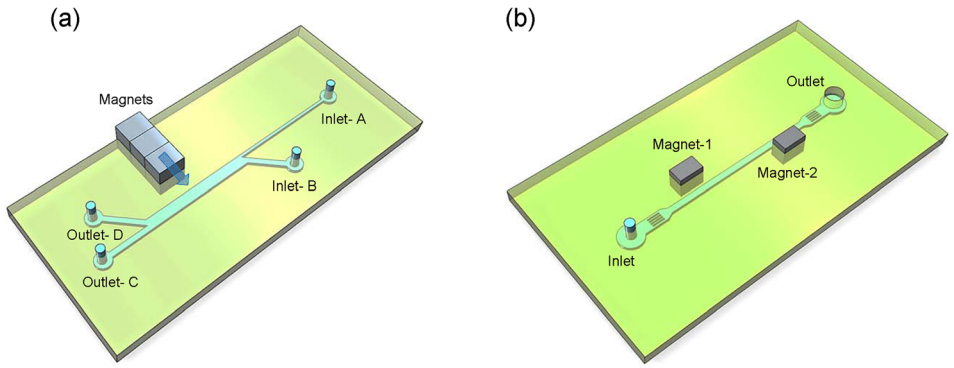

FIG. 7. Separation in microfluidics (a) Sorting of cells by the external magnets based on the magnetophoresis. Reproduced with the permission from Zhu *et al*., Microfluid. Nanofluid. **13**, 645–654 (2012). Copyright 2012 Springer-Verlag. (b) Straight microchannel with a pair of off-set magnets. Reproduced with the permission from Zeng *et al*., J. Magn. Magn. Mater. **346**, 118–123 (2013). Copyright 2013 Elsevier B.V. (Figures are not to scale).

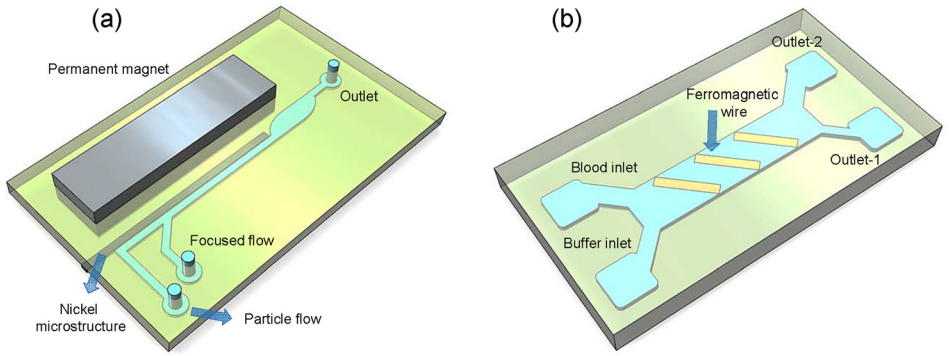

FIG. 8. Separation in microfluidics (a) CTC microchannel integrated with ferromagnetic wire. Separation is initiated by an external magnetic force. Reproduced with the permission from Shen *et al*., Anal. Chem. **84**, 3075–3081 (2012). Copyright 2012 American Chemical Society. (b) Magnetophoretic separation using a repulsive force in a paramagnetic solution. The magnetic field gradient is enhanced by incorporating a micro-nickel structure. Reproduced with the permission from Kim *et al*., Anal. Chem. **85**, 2779–2786 (2013). Copyright 2013 American Chemical Society. (Figures are not to scale).

5 cells per ml from a complex sample such as blood, saliva, or urine.[66] The specifically bound reagent tagged with magnetic beads makes the separation reliable for biological sample identifications. Gourikutty *et al*. demonstrated a two-stage microchip to isolate circulating tumor cells (CTCs) from the whole blood sample, Fig. 6(a).[22] The first stage removed magnetically labeled white blood cells (WBCs) from the blood sample using immune tagging and magnetophoretic separation. Next, the sample is fed into a micro-slit filter to remove the red blood cells (RBCs) according to their sizes. This approach recovered almost 96.8% CTCs from the 2 ml sample in only 50 min. However, this CTC enrichment process has a potential risk of losing target CTCs along with the other blood cells. Further modification of the concept is necessary for clinical applications.

Mizuno *et al*. reported the separation of human lymphocyte cells utilizing the size difference and surface marker expressions, Fig. 6(b).[67] First, the cells were tagged with anti-CD4 conjugated immunomagnetic beads that were then sorted by the size difference. The cells were then focused hydrodynamically. Magnetically tagged cells were then separated by magnetophoresis. A permanent magnet positioned perpendicular to the stream separated the strongly conjugated cell-bead from the rest of the samples. Plouffe *et al*. reported the isolation of immunomagnetically tagged rare MCF-7 cells from the highly concentrated B-lymphocyte cells with an efficiency of almost 85%.[68] Conducting wires serving as electromagnets were aligned beneath the channel bottom. The electromagnets were activated by an external DC current source. The team further extended this work to the isolation of endothelial progenitor cells and the hematopoietic

stem cells from the human blood with an efficiency of 96%. Forbes and Forry developed a microfluidic device to separate immune-magnetically labeled rare mammalian cells from the cell-bead complexes.[69] The angled permanent magnets relative to the flow direction promoted lateral magnetophoresis of the magnetically tagged breast adenocarcinoma (MCF-7) cells. The efficiency of the system was further optimized with the magnet type and orientation, flow rate, and channel geometry. Wong *et al.* demonstrated hydrodynamic focusing and magnetophoretic separation of magnetically tagged HeLa cells.[70] The magnetic field gradient was generated through multilayered current carrying conductors. Separation of the cells was adjusted through the induced magnetic field with an efficiency of 79%. Robert *et al.* studied the separation of monocytes and macrophages through positive magnetophoresis.[21] Both cell lines were internalized with magnetic nanoparticles based on their endocytosis capacity. Different loadings of nanoparticles, ratio of the cell mixture, and a range of flow rates were considered to enhance the separation efficiency. Based on the magnetic loading, the same types of cells can efficiently be sorted. The sorted cells showed a good purity of more than 88%, and an efficiency of more than 60%, respectively.

A number of works are reported for the separation of particles and cells using negative magnetophoresis. Zhu *et al.* demonstrated the separation of 1-μm, 1.9-μm, and 3.1-μm diamagnetic particles from the 9.9-μm particles in a magnetic field gradient.[71] The same group described the continuous separation of particles and live cells (Escherichia coli and Saccharomyces cerevisiae) of different sizes suspended in a ferrofluid, Fig. 7(a).[27] In the magnetic field, large particles and *S. cerevisiae* were deflected from rest of the *E. coli* with a separation efficiency of almost 100%. Zeng *et al.* separated diamagnetic particles and live yeast cells suspended in ferrofluid using a pair of offset magnets, Fig. 7(b).[72] The first magnet focused the mixture, while the second magnet separated them due to the size differences. Deflection can be adjusted by varying the flow rate for both of the particles. Liang and Xuan designed a U-shaped microchannel to focus and separate 5-μm and 15-μm polystyrene particles in a diluted ferrofluid.[73] Sheath-free focusing was achieved at the beginning of the channel. The larger particles were separated from the smaller counterpart, resulting in efficient separation at the end of the channel. In another work, Zhao *et al.* developed a microfluidic device that enriched the CTCs from the patients' blood sample utilizing a biocompatible ferrofluid.[74] The device extracted debris from the blood sample using filters. The larger CTCs were then focused by sheath flow and removed from white blood cells (WBCs) by an external magnetic field. The optimized device showed high throughput (6 ml/h), a high recovery rate (92.9%), and an average purity (11.7%) of the extracted cells.

Focusing of the sample in a microchannel is a prerequisite for efficient separation. The focusing process can be initiated hydrodynamically by sheath streams of buffer solution or ferrofluid solution. The sheath flow pushes the suspended particle into a narrow stream. In a magnetic field, the targeted particles are then separated from the rest of the samples. The inlet channel with grooves can also focus the cell sample without utilizing the sheath-flow. Sheath-free focusing of the sample and their successful separation have been reported in many recent works. For an instance, Zhang *et al.* reported sheathless focusing and magnetophoretic separation of magnetic beads from non-magnetic beads suspended in a ferrofluid.[75] A microchannel with grooves at the bottom focused the magnetic beads (6-μm) at the centre line of the microchannel. Diamagnetic beads (13 μm) were separated and dragged along the sidewall of the channel due to negative magnetophoresis. Successful separation was achieved with a high throughput of 80 μl/min. Zhu *et al.* showed that the coexistence of positive and negative magnetophoresis can be used to separate a particle mixture due to their different magnetic properties.[17] The concentration of magnetic nanoparticles was selected such that the magnetic susceptibility of the ferrofluid lies between those of the particles. As a result, magnetic-diamagnetic separation (2.6-μm from 4.2-μm, and 7.3-μm from 7.9-μm) and magnetic-magnetic separation (2.8-μm from 8.2-μm) of particles with different sizes were achieved successfully.

Size-based separation is not always reliable with magnetophoresis. For instance, separating live cells from dead cells is hard due to their identical sizes. The dead cells may slightly deform but cannot be distinguished by magnetophoresis. Introducing shape based separation may improve the performance. Besides, the shape is an important parameter for investigating

cell synchronization and disease detection. Moreover, the size and shape of the cells may provide important insights into their maturity, cycle, and differentiation capability.[67] The same types of cells could have an identical volume but different shapes. Deformation of cells may occur due to the interruption of the metabolic function caused by a disease.[16] Thus, infected cells can be identified from their healthy counterparts based on their shape. For instance, the shape changes in RBCs could provide an early indication of a disease.[11] Considering both the size and shape, the magnetization could further improve the separation performance of the system. Shape-based separation of particles and cells by magnetophoresis has been reported by a few research groups. Zhou and Xuan demonstrated magnetophoretic separation of the spherical and peanut shaped diamagnetic particles suspended in a ferrofluid.[76] Both particles had an identical volume of almost 118 μm^3. However, the shape variation among the particles led to different magnetic and drag force, resulting in effective separation. The deflection of both particles was optimized for a range of flow rates.

A strong magnetic field gradient could increase the separation efficiency by many folds. The magnetic field gradient could be improved by optimizing the geometry of the magnets. For instance, Xia *et al.* developed microcomb and microneedle structures that focus the magnetic field and increase the field gradient locally. Red blood cells (RBCs) and *E.coli* tagged with magnetic nanoparticles were isolated with a high throughput and high efficiency.[77] The integration of ferromagnetic microstructures can also focus and increase the local magnetic field gradient. A combination of external large permanent magnets and integrated soft-magnetic structures could increase the magnetic field gradient by multiple folds.[78] As an example, Shen *et al.* used gadolinium diethylenetriamine pentaacetic acid (Gd-DTPA) as a paramagnetic medium with different concentrations to separate the U937 cells from the RBCs with a purity of 90%, Fig. 8(a).[79] The integration of micro ferromagnetic nickel structures between the permanent magnets and the channel doubled the magnetic field gradient. Polystyrene beads of 8-μm and 10-μm diameters were separated to validate the sensitivity of the design. Nam *et al.* demonstrated the separation of malaria-infected RBCs (i-RBCs) and healthy RBCs (h-RBCs) based on their paramagnetic properties.[80] Incorporation of a ferromagnetic nickel wire along the microchannel increased the local magnetic field gradient. The team demonstrated the successful separation of early stage i-RBCs with weak paramagnetic characteristics. Kim *et al.* reported the separation of cancer-specific CTCs from human peripheral blood using immunomagnetic nanobeads bound to EpCAM antibodies, Fig. 8(b).[81] A buffer stream was used to focus the diluted blood with spiked CTCs. The isolation performance of the CTCs was improved by integrating a ferromagnetic wire array beneath the surface of the microchannel. Almost 90% of the CTCs were isolated with a high throughput of 5 ml/h with a purity of 97%.

One of the major problems in magnetophoresis is the accumulation of magnetic nanoparticles on the side wall of the microchannel. For long-term operation over many hours, the channel may be completely blocked by the nanoparticles. Introducing a predefined concentration gradient with the co-flowing sample is a new approach to address this issue. The stream with a lower concentration of magnetic nanoparticles is placed close to the higher field strength. The concentration gradient also promotes magnetophoresis. For instance, Zhou and Wang utilized co-flowing water and diluted ferrofluid to focus and separate 7-μm particles from 2-μm particles.[82] Neodymium (NdFeB) powder was mixed with PDMS and inserted into a specially designed microstructure parallel to the channel. Magnetized upon an impulse magnetizer, the microstructure generated a higher magnetic field gradient than a single permanent magnet. The co-flowing fluids established a stable interface between two different magnetic susceptibilities that focused and trapped the large particles. The small particles keep their initial trajectory and thus are separated from the rest of the samples. Zhao *et al.* reported a label-free separation of cancer cells from white blood cells (WBCs).[83] Reducing the exposure time to the ferrofluid ensures the integrity of the cells. In the main channel, the cell sample instantly mixed with the ferrofluid due to the magnetoconvective secondary flow. The cells are deflected from the ferrofluid streams and pass through the buffer solution. Thus, on-chip washing was also introduced. The size-based separation yields an average separation efficiency of 82.2% and an excellent viability of 94%.

C. Magnetophoresis for trapping

On-chip sample processing and investigation require controlled capture and release of target molecules and cells. The target molecules need to be in the chip until they are exposed to the intended reagents. However, the concentrated beads may aggregate and potentially block the flow path.[84] Particles can be trapped for both positives and negative magnetophoresis, so that both paramagnetic and diamagnetic particles can be trapped inside a microchannel. Similar to mixing and separation, the effectiveness of trapping depends on the height and the width of the microchannel, the size and the strength of the magnets, size of the beads and their susceptibility, and fluid viscosity and the flow rates.[85,86] If the magnetic force is dominant over the hydrodynamic drag force, trapping occurs. Trapping zones are field minima or maxima for diamagnetic and magnetic particles, respectively.

Trapping with positive magnetophoresis occurs if the particle has a higher magnetic susceptibility than the surrounding medium.[87] Utilizing positive magnetophoretic, diamagnetic cells can bind to magnetic beads to be trapped at field maxima. Targeted cells are often trapped on the side wall or a designated reservoir of a microchannel. As a consequence, a large bead cluster may form and trap unwanted particles. Thus, for a higher purity, controlled washing and targeted release need to be addressed. Scherr *et al.* utilized positive magnetophoresis to capture protein conjugated biomarkers in a static pre-arrayed fluid cartridge.[88] Surface functionalized magnetic beads were concentrated using a pair of magnets. The two magnets reduced the capture time of the proteins and the surface functionalized magnetic beads. Kirby *et al.* utilized a DC motor to rotate the entire microfluidic platform, Fig. 9(a).[89] Separation and trapping of magnetic and nonmagnetic beads of different sizes were carried out based on centrifugal forces at different rotation speeds. First, the particle mixture was focused on a narrow path. The small 1-μm magnetic particles were deflected toward the reservoir A close to the magnet. The nonmagnetic particle flows in a straight trajectory towards the waste reservoir B. The 20-μm magnetic particles with bound cells flow into the target reservoir C for further analysis.

Teste *et al.* developed a magnetic chamber filled with 6–8 μm ferromagnetic iron beads to trap 30-nm magnetic nanoparticles.[41] At an optimized flow rate, a bead plug was formed as a physical barrier. These magnetic beads also focused the magnetic field that in turns increases the field gradient of the external permanent magnets. Guo *et al.* described the dynamic separation, stationary trapping, and detection of target pathogen (*S. Typhimurium*) on *E.coli* coupled with streptavidin modified magnetic quantum dots (QDs).[90] A controllable electromagnetic field was generated by an array of nickel wire integrated within the microchannel. The magnetically tagged pathogen was separated due to the lateral magnetic force. The separated pathogen was guided towards the patterned nickel array for trapping. The major problem of trapping with positive magnetophoresis is the accumulation of magnetic particles into a cluster. Even after removing the magnetic fields, the bead cluster still remains on the channel surface and blocks

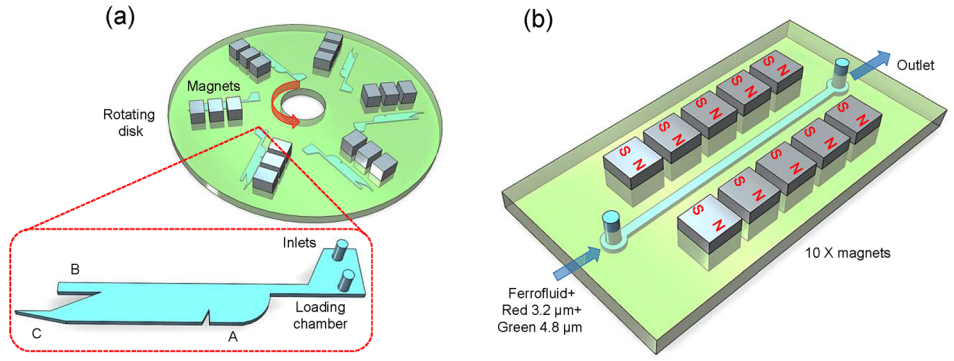

FIG. 9. Trapping in microfluidics (a) Separation and capture of particles through the centrifugo-magnetophoresis. Reproduced with the permission from Kirby *et al.*, Microfluid. Nanofluid. **13**, 899–908 (2012). Copyright 2012 Springer-Verlag. (b) Magnetofluidic concentration and size-selective traps for the diamagnetic particle. Reproduced with permission from Biomicrofluidics **10**, 044103 (2016). Copyright 2016 AIP Publishing LLC. (Figures are not to scale).

the flow. Adjusting the magnetic field gradient may resolve the clogging problem. For instance, Huang *et al.* introduced microwells between the microchannel and the magnets for trapping immunomagnetically labeled THP-1 cells (CD45+Dynabeads labeled cells).[91] The microwell uniformly distributed the magnetic field throughout the trapping channel. Single cells were collected on each microwell with an efficiency of 62% and a purity of 99.6%. Koschwanez *et al.* reported trapping of magnetically labeled single cells in a triangle shaped ferromagnetic element.[92] The element was magnetized by an external permanent magnet. The trapped yeast cells were further investigated for a period of time. The captured force was measured in terms of flow speed. Controlled release of the post analyzed cell showed ample cell visibility. The benefits of a single cell trapped with magnetophoresis are the extended period of investigation without affecting its viability, observing the proliferation and biomarker expression without damaging its integrity, and being inexpensive compared to other methods.[74,83]

Trapping with negative magnetophoresis occurs if the magnetic susceptibility of the particle is lower than that of the surrounding medium. Once the targeted cells are isolated and guided towards a designated spot, on-chip investigation can be proceeded. Trapping of beads and cells by negative magnetophoresis are found in many recent reports. For instance, Hejazian and Nguyen demonstrated trapping of 3.1-μm and 4.8-μm diamagnetic particles suspended in diluted ferrofluid, Fig. 9(b).[93] The smaller particles were trapped at the magnetic field maxima. The large particles were concentrated at the field minima. Different concentrations of ferrofluid and the flow rate ratio were studied to optimize the trapping performance. Winkleman *et al.* demonstrated trapping of diamagnetic objects in a paramagnetic solution (Gd.DTPA) using a three-dimensional (3D) magnetic trap.[94] Cone shaped permanent magnets with opposite polarities were utilized for trapping of polystyrene spheres, living mouse fibroblast, yeast cells, and algae. Wang *et al.* investigated trapping and alignment of bacteria, and beads suspended in a ferrofluid, Fig. 10(a).[36] An island at the center of the microchannel distorted the external magnetic fields. The susceptibility variation was observed on the edge of the island due to the disruption of the suspended ferrofluid. The trapped bacteria and their clusters formed a chain structure based on their size differences. The magnetic field strength, the duration of the applied field, and the flow rate were varied to determine the condition for trapping and controlled release of the bacteria from the rest of the sample. The team extended their work to separate and concentrate bacteria and magnetic nanoparticles on different parts of the island.[95] The magnetic particles were concentrated at the tip of the island. The bacteria were accumulated at the center of the island.

Zhou *et al.* utilized a permanent magnet adjacent to a T-shaped microchannel to trap 9.9-μm diamagnetic and 2.8-μm magnetic particles, Fig. 10(b).[96] Simultaneous trapping of particles indicates the existence of both positive and negative magnetophoresis in a diluted ferrofluid. Peyman *et al.* showed the versatility of the focusing, deflection, and trapping of polystyrene beads just by altering the magnetic field array.[97] The 5-μm and 10-μm particles were focused, trapped, and

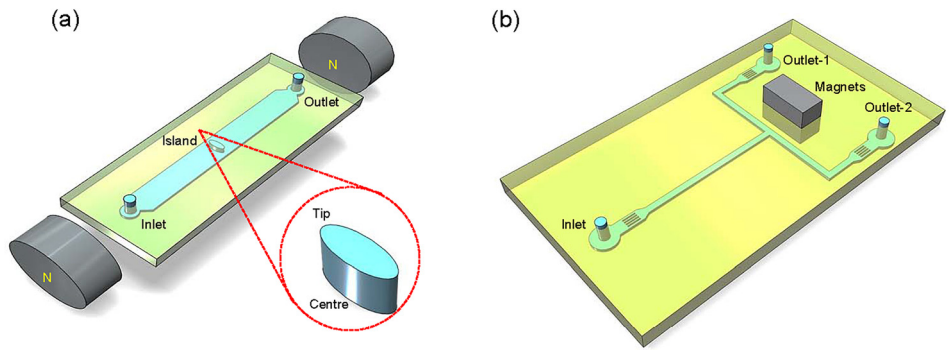

FIG. 10. Trapping in microfluidics (a) A microchannel incorporating an island to trap magnetic particles and bacteria. Reproduced with the permission from Wang *et al.*, Sens. Actuators, B **260**, 657–665 (2018). Copyright 2018 Elsevier B.V. (b) T-shaped microchannel to concentrate and separate the magnetic and diamagnetic particles. Reproduced with the permission from Biomicrofluidics **9**, 044102 (2015). Copyright 2015 AIP Publishing LLC. (Figures are not to scale).

separated throughout the channel for different magnet arrangements and flow rates. A diluted paramagnetic salt solution ($MnCl_2$) was used to initiate magnetophoresis in the microchannel. Zeng *et al*. devised a simple method to concentrate polystyrene particles and live yeast cells suspended in ferrofluid.[98] Two attracting magnets positioned on the opposite sides of a straight microchannel promoted negative magnetophoresis. The flow velocity and the distance between the attracting magnets were adjusted to optimize the trapping performance. Wilbanks *et al*. studied the asymmetric field pattern of magnets and flow rates for trapping 5-μm diamagnetic particles, Fig. 11(a).[99] Magnets positioned around a straight microchannel could increase the trapping performance. The trapped particles rotated in two stable counter rotations within the microchannel due to the asymmetric field pattern of the magnetic arrays. Gertz and Khitun demonstrated trapping of RBCs using magnetite nanoparticles.[100] Manipulation was accomplished with a microelectromagnet consisting two current-carrying wires. Upon the activation, the nanoparticles along with the RBCs move towards the magnetic field minima.

Simultaneous trapping and washing of particles by a rotating magnetic field have also been reported. For instance, Verbarg *et al*. designed a spinning magnetic array that simultaneously traps, washes, and releases the bead-target complex, Fig. 11(b).[101] Six pairs of rectangular magnets rotated under a microchannel. The particles with the targets were trapped and separated from rest of the sample. Controlled release of the target sample was done by reversing the rotation. *E.coli* samples with different concentrations were exposed to the reagent without any aggregation. Ramadan and Gijs demonstrated simultaneous washing and trapping of magnetic particles on a microfluidic chip.[102] The array of magnets rotate under the microchannel for continuous trapping and release of the particles. Impurities within the mixture were released from the target sample by positive magnetophoresis. The design improved reagent binding and reduced processing time.

IV. SIGNIFICANCE AND LIMITATIONS OF MAGNETOPHORESIS

Magnetophoresis has some limitations that need to be addressed carefully. The accumulation of magnetic nanoparticles is an issue for the integrity and proliferation of cells. Cells mixed with a diluted ferrofluid may solve this problem.[61] A longer exposure of the cells to the paramagnetic medium may affect the cell integrity. Parallel fluid flow where the sample may instantly mix with the paramagnetic fluid just before the separation may prevent this problem.[82,83] However, biocompatibility of the paramagnetic solution needs to be controlled for live cell manipulation. In this regard, the pH value, tonicity, and nanoparticle surfactant optimization need to be maintained for colloidal stability.[103] Works have been reported on cell viability

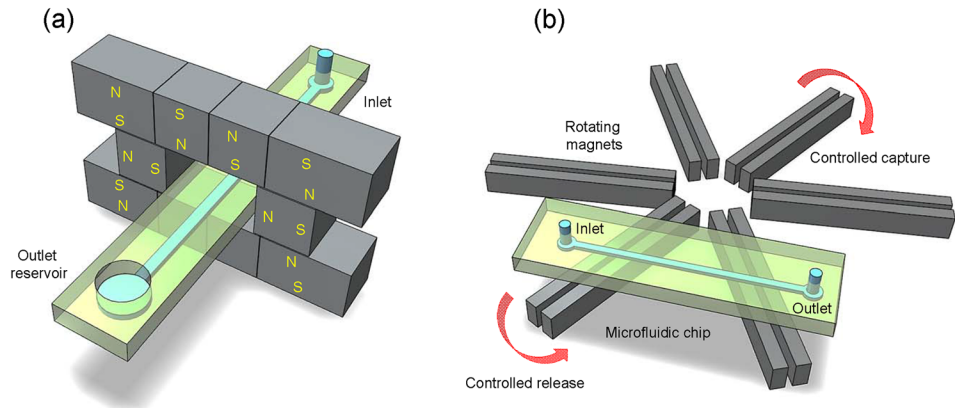

FIG. 11. Trapping in microfluidics (a) three-dimensional magnet array for the concentration of diamagnetic particles. Reproduced with the permission from J. Appl. Phys. **115**, 044907 (2014). Copyright 2014 AIP Publishing LLC. (b) Rotating magnetic field to simultaneously trap and release of magnetic particles. Reproduced with the permission from Verbarg *et al*., Lab Chip **12**, 1793–1799 (2012). Copyright 2012 The Royal Society of Chemistry. (Figures are not to scale).

for up to a few hours. For instance, *E. coli* and *S. cerevisiae* were reported to be viable for 2 h in a commercial water-based ferrofluid.[27] Zhao *et al.* utilized a custom made ferrofluid with a volume fraction of the magnetic content of only 0.26% to separate the CTCs from the whole blood sample using negative magnetophoresis.[74] The ferrofluid was functionalized with a graft copolymer to avoid the accumulation of magnetic nanoparticles. The pH level was adjusted to 7.0 for the biocompatibility. The extracted CTCs showed ample biomarker expression, excellent viability, and good proliferation.

Besides, the viability may vary significantly for mammalian cells of different types, batches, and population. Customizing the paramagnetic solution is essential to improve cell viability. Krebs *et al.* demonstrated the synthesis of biocompatible ferrofluid with bovine serum albumin (BSA) to passivate magnetite nanoparticles for live cell assembly.[104] The modified ferrofluid showed good inertness, cytocompatibility and colloidal stability of the suspended cell assembly. The nanoparticles allow human umbilical vein endothelial cells (HUVECs) to assemble into a linear chain. The cells were exposed to the modified ferrofluid for up to 2 h. More than 95% of the exposed cells were viable. Kose *et al.* utilized 40 mM citrate with biocompatible ferrofluid for the stabilization of cells.[105] Citric acid stabilized the cobalt ferrite nanoparticles and yielded a pH of 7.4 to reduce the toxicity. A simple microfluidic platform was used with an array of conductors to induce a periodic magnetic field. Size based trapping of beads and shape-based concentration of RBCs from the *E. coli* bacteria were performed. Elasticity-based separation of the RBCs from the sickle cells was also investigated. The cells were suspended in the ferrofluid for several hours. More than 75% of the cells were viable after a long exposure to the customized ferrofluid. Separated microparticles and live cells showed improved diagnostic sensitivity. Excellent cell integrity and proliferation have also been reported for a higher volume fraction of the magnetic nanoparticles up to 1%.[106] By stabilizing the magnetic nanoparticles with a graft copolymer and adjusting the pH value to 6.8, mouse blood cells and Hela cells showed a viability up to 100% and 90%, respectively, after 2 h exposure.

Label-free cell manipulation is challenging due to the subtle difference of cells. For instance, HeLa cells, and RBCs may have a volume range of $3700 \pm 1500\ \mu m^3$ and $66 \pm 8.3\ \mu m^3$, respectively.[107,108] WBCs and CTCs have a diameter ranging between 8 and 14 μm, and 15–25 μm, respectively. Even smaller CTCs were found in blood samples.[74] Therefore, the size based separation is not reliable due to the identical volume and density of the cells.[109] Furthermore, processing a large amount of biological sample is challenging due to the limitation of device throughput. Biological samples such as clinically collected blood are difficult to process with magnetophoresis, because blood viscosity depends on the non-uniform distribution of the RBCs.[110] RBCs can easily change their shape and deform under a high shear stress. As a consequence, the drag force and lift force acting on the RBCs also change, affecting the separation results. Furthermore, the device performance may significantly deteriorate due to the high flow resistance.[111] Optimum flow rates, shallow channels, and an optimum channel width to length ratio may minimize the flow resistance. The implementation of other separation physics along with an innovative design may overcome these barriers. As the viscosity of blood changes with temperature, a constant temperature needs to be maintained for the microchip. Tarn *et al.* investigated a wide range of commercial magnetic particles and their magnetophoretic behavior for a range of temperatures.[112] The viscosity of the carrier fluids decreased with increasing temperature. Thus, separation performance may improve with increasing temperature.

V. CONCLUSION AND FUTURE PERSPECTIVE

The ultimate goal for point-of-care diagnostics is designing and implementing simple, rapid, and low-cost devices. Various design parameters are to be considered for the development of a reliable LOC device.[113] Separation and detection are implemented with schemes such as chemical (surface marker), dielectrophoresis (conductance, impedance), and magnetophoresis (susceptibility, volume). Incorporation of the multiple physics into a single LOC device could meet the requirement for a high throughput required for clinical samples. For instance, hydrodynamic filtration can be incorporated together with magnetophoresis. Deterministic lateral

displacement (DLD) may be combined with inertial microfluidics and magnetophoresis for sorting of a clinical sample.[114] Positive and negative magnetophoresis could be used at the same time for handling a wide range of cell types. Multi-physics LOC devices have showed performance enhancement. For instance, Krishnan *et al*. utilized dielectrophoresis to focus the particles of different sizes. Subsequent deflection and trapping of the magnetic particles were implemented with magnetophoresis.[115] The combination of two or more techniques on a single device allowed a more precise manipulation that is difficult with magnetophoresis alone.

The original concept of LOC from the early 1990 was to shrink the entire laboratory and their functionality into a microchip. However, the fluid flow through a bulky external pumping system, image analysis by the expansive microscope, and the subsequent image processing make the true LOC concept difficult to implement. For the portability, bulky syringe pumps and their associated tubing should be avoided. For instance, a push pump and centrifugal pumping are practical solutions for this problem. Laksanasopin *et al*. demonstrated a portable POC unit that operates a fully functional lab-based immunoassay for detecting infectious disease.[116] The device performed a triplexed immunoassay and was powered by a smartphone. The field-level diagnostic results were consistent with the gold standard of the laboratory-based assays. More efforts need to be done to engage clinicians, biologists, or consumers for the adoption of the technology. Product development has to be considered for the end-users rather than demonstrating the proof-of-concept and publishing academic papers.[1] Moreover, the need for complex and expensive apparatus for micromachining is an obstacle towards the rapid and low-cost fabrication of the LOC based on magnetophoresis. 3D printing may offer a fast, cost-effective, and simple fabrication procedure for the microchip fabrication.[117] In the near future, 3D printing might be a practical alternative for conventional soft-lithography, as more complex designs can be implemented at a low cost, as the maintenance of a highly specialized and expensive clean room is no longer needed.

ACKNOWLEDGMENTS

The authors acknowledge funding support from Australian Research Council through Grant No. DP180100055.

[1]G. M. Whitesides, Nature **442**(7101), 368 (2006).
[2]M. Hejazian, W. Li, and N.-T. Nguyen, Lab Chip **15**(4), 959–970 (2015).
[3]N. Pamme, Lab Chip **6**(1), 24–38 (2006).
[4]G. Zhu and N. Trung Nguyen, Micro Nanosyst. **2**(3), 202–216 (2010).
[5]W. Zhao, R. Cheng, J. R. Miller, and L. Mao, Adv. Funct. Mater. **26**(22), 3916–3932 (2016).
[6]C. Yi, C.-W. Li, S. Ji, and M. Yang, Anal. Chim. Acta **560**(1-2), 1–23 (2006).
[7]P. Sajeesh and A. K. Sen, Microfluid. Nanofluid. **17**(1), 1–52 (2014).
[8]N. Pamme, J. C. Eijkel, and A. Manz, J. Magn. Magn. Mater. **307**(2), 237–244 (2006).
[9]A. Munaz, B.-C. Lee, and G.-S. Chung, Sens. Actuators, A **201**, 134–140 (2013).
[10]A. Munaz and G.-S. Chung, Microsyst. Technol. **23**, 91–99 (2017).
[11]S. Huang, H. Yong-Qing, and J. Feng, Chin. J. Anal. Chem. **45**(8), 1238–1246 (2017).
[12]N.-T. Nguyen, Microfluid. Nanofluid. **12**(1-4), 1–16 (2012).
[13]I. Šafařík and M. Šafaříková, J. Chromatogr. B **722**(1-2), 33–53 (1999).
[14]J. Nilsson, M. Evander, B. Hammarström, and T. Laurell, Anal. Chim. Acta **649**(2), 141–157 (2009).
[15]J. Faraudo, J. S. Andreu, and J. Camacho, Soft Matter **9**(29), 6654–6664 (2013).
[16]Y. Chen, P. Li, P.-H. Huang, Y. Xie, J. D. Mai, L. Wang, N.-T. Nguyen, and T. J. Huang, Lab Chip **14**(4), 626–645 (2014).
[17]T. Zhu, R. Cheng, Y. Liu, J. He, and L. Mao, Microfluid. Nanofluid. **17**(6), 973–982 (2014).
[18]N. Pamme and C. Wilhelm, Lab Chip **6**(8), 974–980 (2006).
[19]H. W. Child, P. A. del Pino, J. M. De La Fuente, A. S. Hursthouse, D. Stirling, M. Mullen, G. M. McPhee, C. Nixon, V. Jayawarna, and C. C. Berry, ACS Nano **5**(10), 7910–7919 (2011).
[20]T. Salafi, K. K. Zeming, and Y. Zhang, Lab Chip **17**(1), 11–33 (2017).
[21]D. Robert, N. Pamme, H. Conjeaud, F. Gazeau, A. Iles, and C. Wilhelm, Lab Chip **11**(11), 1902–1910 (2011).
[22]S. B. N. Gourikutty, C.-P. Chang, and P. D. Puiu, J. Chromatogr. B **1011**, 77–88 (2016).
[23]G.-P. Zhu, M. Hejiazan, X. Huang, and N.-T. Nguyen, Lab Chip **14**(24), 4609–4615 (2014).
[24]A. Skjeltorp, Phys. Rev. Lett. **51**(25), 2306 (1983).
[25]R. E. Rosensweig, *Ferrohydrodynamics* (Courier Corporation, 2013).
[26]M. Hejazian and N.-T. Nguyen, Lab Chip **15**(14), 2998–3005 (2015).
[27]T. Zhu, R. Cheng, S. A. Lee, E. Rajaraman, M. A. Eiteman, T. D. Querec, E. R. Unger, and L. Mao, Microfluid. Nanofluid. **13**(4), 645–654 (2012).
[28]L. Liang, C. Zhang, and X. Xuan, Appl. Phys. Lett. **102**(23), 234101 (2013).

[29]J. Vanderlinde, *Classical Electromagnetic Theory* (Springer Science & Business Media, 2006).
[30]P. M. Gresho and R. L. Sani, *Incompressible Flow and the Finite Element Method, Volume 1: Advection-diffusion and Isothermal Laminar Flow* (John Wiley and Sons, Inc., New Jersey, 1998).
[31]L. D. Landau and E. M. Lifshitz, *Fluid mechanics, Volume 6: Course of Theoretical Physics* (Pergamon Press, Oxford, 1987).
[32]R. Cheng, T. Zhu, and L. Mao, Microfluid. Nanofluid. **16**(6), 1143–1154 (2014).
[33]A. Munaz, R. K. Vadivelu, J. A. St John, and N.-T. Nguyen, Lab Chip **16**(15), 2946–2954 (2016).
[34]E. A. Mansur, Y. Mingxing, W. Yundong, and D. Youyuan, Chin. J. Chem. Eng. **16**(4), 503–516 (2008).
[35]G. S. Jeong, S. Chung, C.-B. Kim, and S.-H. Lee, Analyst **135**(3), 460–473 (2010).
[36]Y. Wang, R. Wu, V. B. Varma, Z. Wang, Y. Seah, Z. Wang, and R. Ramanujan, Sens. Actuators, B **260**, 657–665 (2018).
[37]C. W. Shields IV, C. D. Reyes, and G. P. López, Lab Chip **15**(5), 1230–1249 (2015).
[38]C.-Y. Lee, C.-L. Chang, Y.-N. Wang, and L.-M. Fu, Int. J. Mol. Sci. **12**(5), 3263–3287 (2011).
[39]N.-T. Nguyen and Z. Wu, J. Micromech. Microeng. **15**(2), R1 (2004).
[40]T. F. Kong and N.-T. Nguyen, Microsyst. Technol. **21**(3), 519–526 (2015).
[41]B. Teste, F. Malloggi, A.-L. Gassner, T. Georgelin, J.-M. Siaugue, A. Varenne, H. Girault, and S. Descroix, Lab Chip **11**(5), 833–840 (2011).
[42]T. F. Kong, W. K. Peng, T. D. Luong, N.-T. Nguyen, and J. Han, Lab Chip **12**(2), 287–294 (2012).
[43]R. Ganguly, T. Hahn, and S. Hardt, Microfluid. Nanofluid. **8**(6), 739–753 (2010).
[44]G.-P. Zhu and N.-T. Nguyen, Microfluid. Nanofluid. **13**(4), 655–663 (2012).
[45]G.-P. Zhu and N.-T. Nguyen, Lab Chip **12**(22), 4772–4780 (2012).
[46]Z. Wang, V. Varma, H. M. Xia, Z. Wang, and R. V. Ramanujan, Phys. Fluids **27**(5), 052004 (2015).
[47]T. Lund-Olesen, B. B. Buus, J. G. Howalt, and M. F. Hansen, J. Appl. Phys. **103**(7), 07E902 (2008).
[48]M. D. Tarn, R. F. Fakhrullin, V. N. Paunov, and N. Pamme, Mater. Lett. **95**, 182–185 (2013).
[49]M. Hejazian and N.-T. Nguyen, Micromachines **8**(2), 37 (2017).
[50]T.-H. Tsai, D.-S. Liou, L.-S. Kuo, and P.-H. Chen, Sens. Actuators, A **153**(2), 267–273 (2009).
[51]D. Nouri, A. Zabihi-Hesari, and M. Passandideh-Fard, Sens. Actuators, A **255**, 79–86 (2017).
[52]H. Suzuki, C.-M. Ho, and N. Kasagi, J. Microelectromech. Syst. **13**(5), 779–790 (2004).
[53]Y. Wang, J. Zhe, B. T. Chung, and P. Dutta, Microfluid. Nanofluid. **4**(5), 375–389 (2008).
[54]S. H. Lee, D. van Noort, J. Y. Lee, B.-T. Zhang, and T. H. Park, Lab Chip **9**(3), 479–482 (2009).
[55]K. S. Ryu, K. Shaikh, E. Goluch, Z. Fan, and C. Liu, Lab Chip **4**(6), 608–613 (2004).
[56]L.-H. Lu, K. S. Ryu, and C. Liu, J. Microelectromech. Syst. **11**(5), 462–469 (2002).
[57]D.-W. Oh, J. S. Jin, J. H. Choi, H.-Y. Kim, and J. S. Lee, J. Micromech. Microeng. **17**(10), 2077 (2007).
[58]A. Munir, J. Wang, Z. Zhu, and H. S. Zhou, IEEE Trans. Nanotechnol. **10**(5), 953–961 (2011).
[59]A. Rida and M. Gijs, Anal. Chem. **76**(21), 6239–6246 (2004).
[60]S. L. Biswal and A. P. Gast, Anal. Chem. **76**(21), 6448–6455 (2004).
[61]A. Munaz, H. Kamble, M. J. Shiddiky, and N.-T. Nguyen, RSC Adv. **7**(83), 52465–52474 (2017).
[62]N. Veldurthi, S. Chandel, T. Bhave, and D. Bodas, Sens. Actuators, B **212**, 419–424 (2015).
[63]N. Veldurthi, P. Ghoderao, S. Sahare, V. Kumar, D. Bodas, A. Kulkarni, and T. Bhave, Mater. Sci. Eng.: C **68**, 455–464 (2016).
[64]D. Owen, M. Ballard, A. Alexeev, and P. J. Hesketh, Sens. Actuators, A **251**, 84–91 (2016).
[65]N. Azimi and M. Rahimi, J. Magn. Magn. Mater. **422**, 188–196 (2017).
[66]N. Pamme, Curr. Opin. Chem. Biol. **16**(3-4), 436–443 (2012).
[67]M. Mizuno, M. Yamada, R. Mitamura, K. Ike, K. Toyama, and M. Seki, Anal. Chem. **85**(16), 7666–7673 (2013).
[68]B. D. Plouffe, M. Mahalanabis, L. H. Lewis, C. M. Klapperich, and S. K. Murthy, Anal. Chem. **84**(3), 1336–1344 (2012).
[69]T. P. Forbes and S. P. Forry, Lab Chip **12**(8), 1471–1479 (2012).
[70]Q. Y. Wong, N. Liu, C.-G. Koh, H.-Y. Li, and W. S. Lew, Microfluid. Nanofluid. **20**(10), 139 (2016).
[71]T. Zhu, F. Marrero, and L. Mao, Microfluid. Nanofluid. **9**(4-5), 1003–1009 (2010).
[72]J. Zeng, Y. Deng, P. Vedantam, T.-R. Tzeng, and X. Xuan, J. Magn. Magn. Mater. **346**, 118–123 (2013).
[73]L. Liang and X. Xuan, Biomicrofluidics **6**(4), 044106 (2012).
[74]W. Zhao, R. Cheng, B. D. Jenkins, T. Zhu, N. E. Okonkwo, C. E. Jones, M. B. Davis, S. K. Kavuri, Z. Hao, and C. Schroeder, Lab Chip **17**(18), 3097–3111 (2017).
[75]S. Yan, J. Zhang, D. Yuan, Q. Zhao, J. Ma, and W. Li, Appl. Phys. Lett. **109**(21), 214101 (2016).
[76]Y. Zhou and X. Xuan, Appl. Phys. Lett. **109**(10), 102405 (2016).
[77]N. Xia, T. P. Hunt, B. T. Mayers, E. Alsberg, G. M. Whitesides, R. M. Westervelt, and D. E. Ingber, Biomed. Microdevices **8**(4), 299 (2006).
[78]N. Pamme, Lab Chip **7**(12), 1644–1659 (2007).
[79]F. Shen, H. Hwang, Y. K. Hahn, and J.-K. Park, Anal. Chem. **84**(7), 3075–3081 (2012).
[80]J. Nam, H. Huang, H. Lim, C. Lim, and S. Shin, Anal. Chem. **85**(15), 7316–7323 (2013).
[81]S. Kim, S.-I. Han, M.-J. Park, C.-W. Jeon, Y.-D. Joo, I.-H. Choi, and K.-H. Han, Anal. Chem. **85**(5), 2779–2786 (2013).
[82]R. Zhou and C. Wang, Biomicrofluidics **10**(3), 034101 (2016).
[83]W. Zhao, R. Cheng, S. H. Lim, J. R. Miller, W. Zhang, W. Tang, J. Xie, and L. Mao, Lab Chip **17**(13), 2243–2255 (2017).
[84]G. Richardson, K. Kaouri, and H. Byrne, Eur. J. Appl. Math. **21**(1), 77–107 (2010).
[85]R.-J. Yang, H.-H. Hou, Y.-N. Wang, and L.-M. Fu, Sens. Actuators, B **224**, 1–15 (2016).
[86]K. Nandy, S. Chaudhuri, R. Ganguly, and I. K. Puri, J. Magn. Magn. Mater. **320**(7), 1398–1405 (2008).
[87]M. Frenea-Robin, H. Chetouani, N. Haddour, H. Rostaing, J. Laforet, and G. Reyne, paper presented at *30th Annual International Conference of the IEEE Engineering in Medicine and Biology Society, EMBS 2008* (2008).
[88]T. F. Scherr, H. B. Ryskoski, A. B. Doyle, and F. R. Haselton, Biomicrofluidics **10**(2), 024118 (2016).
[89]D. Kirby, J. Siegrist, G. Kijanka, L. Zavattoni, O. Sheils, J. O'Leary, R. Burger, and J. Ducrée, Microfluid. Nanofluid. **13**(6), 899–908 (2012).

[90]P.-L. Guo, M. Tang, S.-L. Hong, X. Yu, D.-W. Pang, and Z.-L. Zhang, Biosens. Bioelectron. **74**, 628–636 (2015).
[91]N.-T. Huang, Y.-J. Hwong, and R. L. Lai, Microfluid. Nanofluid. **22**(2), 16 (2018).
[92]J. H. Koschwanez, R. H. Carlson, and D. R. Meldrum, Rev. Sci. Instrum. **78**(4), 044301 (2007).
[93]M. Hejazian and N.-T. Nguyen, Biomicrofluidics **10**(4), 044103 (2016).
[94]A. Winkleman, K. L. Gudiksen, D. Ryan, G. M. Whitesides, D. Greenfield, and M. Prentiss, Appl. Phys. Lett. **85**(12), 2411–2413 (2004).
[95]Z. Wang, R. Wu, Z. Wang, and R. Ramanujan, Sci. Rep. **6**, 26945 (2016).
[96]Y. Zhou, D. T. Kumar, X. Lu, A. Kale, J. DuBose, Y. Song, J. Wang, D. Li, and X. Xuan, Biomicrofluidics **9**(4), 044102 (2015).
[97]S. A. Peyman, E. Y. Kwan, O. Margarson, A. Iles, and N. Pamme, J. Chromatogr. A **1216**(52), 9055–9062 (2009).
[98]J. Zeng, C. Chen, P. Vedantam, T.-R. Tzeng, and X. Xuan, Microfluid. Nanofluid. **15**(1), 49–55 (2013).
[99]J. J. Wilbanks, G. Kiessling, J. Zeng, C. Zhang, T.-R. Tzeng, and X. Xuan, J. Appl. Phys. **115**(4), 044907 (2014).
[100]F. Gertz and A. Khitun, AIP Adv. **6**(2), 025308 (2016).
[101]J. Verbarg, K. Kamgar-Parsi, A. R. Shields, P. B. Howell, and F. S. Ligler, Lab Chip **12**(10), 1793–1799 (2012).
[102]Q. Ramadan and M. A. Gijs, Procedia Chem. **1**(1), 1499–1502 (2009).
[103]T. Zhu, D. J. Lichlyter, M. A. Haidekker, and L. Mao, Microfluid. Nanofluid. **10**(6), 1233–1245 (2011).
[104]M. D. Krebs, R. M. Erb, B. B. Yellen, B. Samanta, A. Bajaj, V. M. Rotello, and E. Alsberg, Nano Lett. **9**(5), 1812–1817 (2009).
[105]A. R. Kose, B. Fischer, L. Mao, and H. Koser, Proc. Natl. Acad. Sci. **106**(51), 21478–21483 (2009).
[106]W. Zhao, T. Zhu, R. Cheng, Y. Liu, J. He, H. Qiu, L. Wang, T. Nagy, T. D. Querec, and E. R. Unger, Adv. Funct. Mater. **26**(22), 3990–3998 (2016).
[107]T. T. Puck, P. I. Marcus, and S. J. Cieciura, J. Exp. Med. **103**(2), 273–284 (1956).
[108]K. de Jong, R. K. Emerson, J. Butler, J. Bastacky, N. Mohandas, and F. A. Kuypers, Blood **98**(5), 1577–1584 (2001).
[109]S. Suresh, J. Spatz, J. Mills, A. Micoulet, M. Dao, C. Lim, M. Beil, and T. Seufferlein, Acta Biomater. **1**(1), 15–30 (2005).
[110]X. Lu, C. Liu, G. Hu, and X. Xuan, J. Colloid Interface Sci. **500**, 182–201 (2017).
[111]J. Kim and C.-N. Kim, J. Mech. Sci. Technol. **29**(11), 4833–4839 (2015).
[112]M. D. Tarn, S. A. Peyman, D. Robert, A. Iles, C. Wilhelm, and N. Pamme, J. Magn. Magn. Mater. **321**(24), 4115–4122 (2009).
[113]M. Antfolk and T. Laurell, Anal. Chim. Acta **965**, 9–35 (2017).
[114]E. Ozkumur, A. M. Shah, J. C. Ciciliano, B. L. Emmink, D. T. Miyamoto, E. Brachtel, M. Yu, P-i Chen, B. Morgan, and J. Trautwein, Sci. Transl. Med. **5**(179), 179ra147–179ra147 (2013).
[115]J. N. Krishnan, C. Kim, H. J. Park, J. Y. Kang, T. S. Kim, and S. K. Kim, Electrophoresis **30**(9), 1457–1463 (2009).
[116]T. Laksanasopin, T. W. Guo, S. Nayak, A. A. Sridhara, S. Xie, O. O. Olowookere, P. Cadinu, F. Meng, N. H. Chee, and J. Kim, Sci. Transl. Med. **7**(273), 273re271–273re271 (2015).
[117]A. Munaz, R. K. Vadivelu, J. S. John, M. Barton, H. Kamble, and N.-T. Nguyen, J. Sci.: Adv. Mater. Devices **1**(1), 1–17 (2016).